

International Journal of Quantum Information  
Vol. 9, Suppl. (2011) 63–71  
© World Scientific Publishing Company  
DOI: [10.1142/S0219749911007046](https://doi.org/10.1142/S0219749911007046)



## DECAY OF NONLOCALITY DUE TO ADIABATIC AND QUANTUM NOISE IN THE SOLID STATE

B. BELLOMO\*, G. COMPAGNO\*, A. D'ARRIGO<sup>†</sup>, G. FALCI<sup>‡</sup>,  
R. LO FRANCO\*<sup>‡</sup> and E. PALADINO<sup>†</sup><sup>§</sup>

\**CNISM & Dipartimento di Scienze Fisiche  
ed Astronomiche, Università di Palermo,  
via Archirafi 36, 90123 Palermo, Italy*

<sup>†</sup>*Dipartimento di Metodologie Fisiche  
e Chimiche, Università di Catania,  
viale A. Doria 6, 95125 Catania,  
Italy & CNR - IMM MATIS*

<sup>‡</sup>*lofranco@fisica.unipa.it*

<sup>§</sup>*epaladino@dmfci.unict.it*

Received 24 August 2010

We study the decay of quantum nonlocality, identified by the violation of the Clauser-Horne-Shimony-Holt (CHSH) Bell inequality, for two noninteracting Josephson qubits subject to independent baths with broadband spectra typical of solid state nanodevices. The bath noise can be separated in an adiabatic (low-frequency) and in a quantum (high-frequency) part. We point out the qualitative different effects on quantum nonlocal correlations induced by adiabatic and quantum noise. A quantitative analysis is performed for typical noise figures in Josephson systems. Finally we compare, for this system, the dynamics of nonlocal correlations and of entanglement.

*Keywords:* Nonlocality; open quantum systems; Josephson charge qubits.

### 1. Introduction

The presence of quantum correlations in composite nanosystems is an essential resource for quantum information processing.<sup>1</sup> Amongst the most relevant aspects of quantum correlations, of both fundamental and applicative role, are: entanglement,<sup>2</sup> quantum discord<sup>3</sup> and nonlocality.<sup>1,4,5</sup> Studying these quantities for realistic quantum systems that are promising candidates for realizing a quantum computer is an interesting issue. Considerable development has been recently made towards the implementation of a solid-state quantum computer. In particular, superconducting high-fidelity<sup>6–10</sup> single qubit gates with coherence times of  $\sim 1\mu\text{s}$  are now available.<sup>11,12</sup> Two-qubit logic gates have been proved in different laboratories<sup>13–15</sup> and Bell states have been prepared up to 75% of fidelity.<sup>16–19</sup> In a circuit quantum electrodynamic framework, highly entangled two-qubit states with concurrence up to

94% have been also generated, allowing the first implementation of basic quantum algorithms with a superconducting quantum processor.<sup>20</sup>

In order to process quantum information, it is important to establish how long the relevant quantum correlations can be maintained in noisy nanocircuits. Solid state noise may indeed represent a serious limitation towards this goal. Josephson junction-based experimental setups are often influenced by broadband and structured noise, whose typical power spectra show a  $1/f$  low-frequency behavior up to some cut-off frequency followed by a white or ohmic behavior.<sup>21–23</sup> The presence of slow components in the environment makes the decay of the coherent signal strongly dependent on the experimental protocol being used.<sup>12,24</sup> Measurement protocols requiring numerous repetitions are particularly sensitive to the unstable device calibration due to low-frequency fluctuations. The main effect is dephasing due to defocusing of the measured signal. Incoherent energy exchanges between system and environment, leading to relaxation and decoherence, occur at typical operating frequencies (about 10 GHz) where noise is white or ohmic.

Low- and high-frequency noise affects quite differently single-qubit gates: adiabatic (low-frequency) noise typically leads to algebraic decay, while quantum (high-frequency) noise to exponential behavior.<sup>21,24</sup> It is therefore important to evaluate the effect on quantum correlations time evolution of adiabatic noise and of its interplay with quantum noise. This analysis has been recently addressed in detail for entanglement.<sup>25</sup> Here we extend this study to the aspect of nonlocality.

Nonlocal correlations, i.e. correlations not reproducible in the framework of Bell inequality tests by any classical local model, are particularly important for quantum cryptography purposes.<sup>26</sup> In this paper, we consider two noninteracting qubits subject to independent environments with typical broadband spectra. We use the Clauser-Horne-Shimony-Holt (CHSH) inequality and the maximum of the related Bell function<sup>4,5,27</sup> to identify nonlocal correlations for classes of entangled initial states currently obtainable in laboratory. In particular, we study the sensitivity of the time evolution of nonlocal correlations to the initial state purity and degree of entanglement.

## 2. Model

We consider a system composed by two identical superconducting qubits, namely  $A$  and  $B$ , each interacting with independent baths characterized by a broadband spectrum. The total Hamiltonian is  $H_{\text{tot}} = H_A + H_B$ , where each single-qubit Hamiltonian is given by ( $\hbar = 1$ )<sup>24,25</sup>

$$H_\alpha = H_{Q,\alpha} - \hat{\xi}_\alpha \sigma_{z,\alpha}/2, \quad H_{Q,\alpha} = -\vec{\Omega}_\alpha \cdot \vec{\sigma}_\alpha/2, \quad (1)$$

where  $H_{Q,\alpha}$  refers to the qubit  $\alpha = A, B$ ,  $\vec{\sigma}_\alpha$  is the Pauli matrices vector,  $|\vec{\Omega}_\alpha| \equiv \Omega_\alpha$  the qubit frequency splitting and  $\hat{\xi}_\alpha$  are collective environmental variables whose power spectra are  $1/f$  at  $f \in [\gamma_m, \gamma_M]$  (low-frequency noise) and white or ohmic at frequencies of the order of the qubit splittings (high-frequency noise). According to a

standard model, noise with  $1/f$  spectrum can be originated by an ensemble of bistable fluctuators (BFs).<sup>28</sup> The physical origin of the fluctuators depends on the specific setup. For instance, charge based devices are extremely sensitive to background charge fluctuations.<sup>24,29–31</sup> Noise at higher frequencies instead may either originate from quantum impurities,<sup>22,23</sup> possibly of the same physical origin, or being due to the circuitry.

Effects of the different parts of the spectrum can be treated in a multi-stage approach introduced in Ref. 24. Effects of low- and high-frequency components of the noise are distinguished by decomposing  $\hat{\xi}_\alpha \rightarrow \xi_\alpha(t) + \hat{\xi}_{f,\alpha}$ .<sup>32</sup> Stochastic variables  $\xi_\alpha(t)$  describe low-frequency  $1/f$  noise, and can be treated in the adiabatic and longitudinal approximation. High-frequency ( $\omega \sim \Omega_\alpha$ ) fluctuations  $\hat{\xi}_{f,\alpha}$  are modeled by a Markovian bath mainly leading to spontaneous decay. Therefore, populations relax due to quantum noise ( $T_1$ -type times), which also leads to secular dephasing ( $T_2 = 2T_1$ -type). Low-frequency noise provides a defocusing mechanism determining further coherences decay. In the Hamiltonian of Eq. (1), both the operating point (angle  $\theta_\alpha$  between  $z$  and  $\vec{\Omega}_\alpha$ ) and the qubit splitting  $\Omega_\alpha$  are tunable. In the following we will consider both qubit operating at the optimal working point,  $\theta_\alpha = \pi/2$ , where partial reduction of defocusing is achieved.<sup>12,21</sup> In addition we will focus on the case of identical qubits  $\Omega_\alpha \equiv \Omega$ .

The two-qubit density matrix elements will be evaluated in the computational basis  $\mathcal{B} = \{|1\rangle \equiv |11\rangle, |2\rangle \equiv |01\rangle, |3\rangle \equiv |10\rangle, |4\rangle \equiv |00\rangle\}$ , where for each qubit we have  $H_{Q,\alpha}|0\rangle = -(\Omega/2)|0\rangle$ ,  $H_{Q,\alpha}|1\rangle = (\Omega/2)|1\rangle$ . Each subsystem “qubit + environment” evolves independently so that, once known the single-qubit dynamics,<sup>24</sup> the evolved two-qubit density matrix will be readily obtained by a procedure reported in Refs. 33, 34.

### 3. Maximum of the Bell Function

In this section we report the expression of the maximum of the Bell function for the class of two-qubit states whose density matrix  $\hat{\rho}_X$ , in the standard computational basis  $\mathcal{B}$ , has a “X structure”, i.e.

$$\hat{\rho}_X = \begin{pmatrix} \rho_{11} & 0 & 0 & \rho_{14} \\ 0 & \rho_{22} & \rho_{23} & 0 \\ 0 & \rho_{23}^* & \rho_{33} & 0 \\ \rho_{14}^* & 0 & 0 & \rho_{44} \end{pmatrix}. \quad (2)$$

This class of states is general enough to include the most common two-qubit states, like Bell states (pure two-qubit maximally entangled states) and Werner states (mixture of Bell states).<sup>1,2,34</sup> Such a  $X$  form density matrix may arise in a variety of physical situations.<sup>35–37</sup> A further remarkable feature of  $X$  states is that, under various kinds of dynamics, their structure is maintained during time evolution.<sup>33,34</sup>

Using the Horodecki criterion,<sup>27,38</sup> the maximum of the Bell function can be expressed in terms of three functions  $u_1$ ,  $u_2$  and  $u_3$  of the density matrix elements as

$B = 2\sqrt{\max_{j>k}\{u_j + u_k\}}$ , where  $j, k = 1, 2, 3$ . The CHSH inequality reads like  $B \leq 2$ , so that no classical local models are admitted for states such that  $B$  is larger than the classical threshold 2. The three functions  $u_j$  are<sup>38,39</sup>

$$u_1 = 4(|\rho_{14}| + |\rho_{23}|)^2, \quad u_2 = (\rho_{11} + \rho_{44} - \rho_{22} - \rho_{33})^2, \quad u_3 = 4(|\rho_{14}| - |\rho_{23}|)^2. \quad (3)$$

Being  $u_1$  always larger than  $u_3$ , the maximum of the Bell function for X states is

$$B = \max\{B_1, B_2\}, \quad B_1 = 2\sqrt{u_1 + u_2}, \quad B_2 = 2\sqrt{u_1 + u_3}. \quad (4)$$

This quantity has already been studied in dynamical contexts of independent qubits each coupled to a bosonic reservoir (cavity) with Markovian<sup>40</sup> and non-Markovian<sup>41</sup> characteristics. In the following, we shall investigate the maximum of the Bell function,  $B$ , for our system of two independent Josephson qubits each interacting with individual baths.

#### 4. Initial States

We consider extended Werner-like (EWL) two-qubit initial states<sup>34</sup>

$$\hat{\rho}^\Phi = r|\Phi\rangle\langle\Phi| + (1-r)I_4/4, \quad \hat{\rho}^\Psi = r|\Psi\rangle\langle\Psi| + (1-r)I_4/4, \quad (5)$$

whose pure parts are the one/two-excitation Bell-like states  $|\Phi\rangle = a|01\rangle + b|10\rangle$ ,  $|\Psi\rangle = a|00\rangle + b|11\rangle$ , where  $|a|^2 + |b|^2 = 1$ . The purity parameter  $r$  quantifies the mixedness and  $a$  sets the degree of entanglement of the initial state. The density matrix of EWL states, in the computational basis, is non-vanishing only along the diagonal and anti-diagonal ( $X$  form) and this structure is maintained at  $t > 0$  in the system we are considering. Using concurrence<sup>42</sup>  $C$  to quantify entanglement, one can also notice that the initial entanglement is equal for both the EWL states of Eq. (5) and reads  $C_\rho^\Phi(0) = C_\rho^\Psi(0) = 2\max\{0, (|ab| + 1/4)r - 1/4\}$ . Initial states are thus entangled for  $r > r^* = (1 + 4|ab|)^{-1}$ .

Entangled states with purity  $\approx 0.87$  and fidelity to ideal Bell states  $\approx 0.90$  have been experimentally generated.<sup>20</sup> These states may be approximately described as EWL states with  $r_{\text{exp}} \approx 0.91$ .

#### 5. Time Behavior of the Maximum of the Bell Function

In this section, we shall analyze the dynamics of the maximum of the Bell function,  $B$  of Eq. (4), initially considering the case when only adiabatic noise is present and in a second stage including the effect of quantum noise. We shall also compare the dynamics of  $B$  and of the concurrence  $C$ .

##### 5.1. Adiabatic noise

The effect of low-frequency noise components is obtained by the Hamiltonian Eq. (1) with  $\hat{\xi} \approx \xi(t)$  treated in the adiabatic and longitudinal approximation, for which

single-qubit populations do not evolve in time.<sup>24,25</sup> The main effect of low-frequency fluctuations is dephasing due to defocusing processes. The leading order effect depends only on the noise variance, which can be estimated by independent measurements of the amplitude of the  $1/f$  power spectrum on the uncoupled qubits, as follows  $S^{1/f}(\omega) = \pi\Sigma^2[\ln(\gamma_M/\gamma_m)\omega]^{-1}$ . By exploiting the single-qubit coherences determined in this case,<sup>24</sup> we can construct the two-qubit density matrix<sup>33,25</sup> at time  $t$ . Choosing initial states of the form (5)  $B$  is obtained from Eq. (4).

We find that, under adiabatic noise,  $B(t) \equiv B_{\text{ad}}(t)$  is the same for both the initial EWL states of Eq. (5). The explicit expressions of  $B_{\text{ad}}(t)$  and of the times when  $B_{\text{ad}} = 2$ , that is when a Bell inequality “violation sudden death” (VSD) occurs, are given by

$$B_{\text{ad}}(t) = 2r\sqrt{1 + \frac{4|ab|^2\Omega^2}{\Omega^2 + \Sigma^4 t^2}}, \quad t_{\text{VSD}}^{\text{ad}} = \frac{\Omega}{\Sigma^2} \sqrt{\frac{4|ab|^2 r^2}{(1-r)^2} - 1}. \quad (6)$$

For any  $r < 1$ , the Bell inequality is violated at a finite time. Instead, for pure initial entangled states ( $r = 1$ ),  $B_{\text{ad}}(t)$  approaches asymptotically the classical threshold. The evolution of  $B_{\text{ad}}(t)$  is displayed in Fig. 1 for  $\Sigma/\Omega = 0.02$ , which is a typical figure of  $1/f$  noise in single-qubit experiments.<sup>12,21,24</sup> The dependence on the initial degree of entanglement, parameterized by  $|a|^2$ , for fixed  $r = 0.9$ , is reported in panel (a). Sensitivity to the initial purity  $r$ , for fixed  $a = 1/\sqrt{2}$ , is shown in panel (b). We note that the maintenance of nonlocal correlations ( $B > 2$ ) strongly depends on the purity of the initial state  $r$ , while the dependence on  $|a|^2$  is weaker and symmetric around  $|a|^2 = 1/2$ . The “violation sudden death” of  $B_{\text{ad}}(t)$  for  $r < 1$  is also clearly visible.

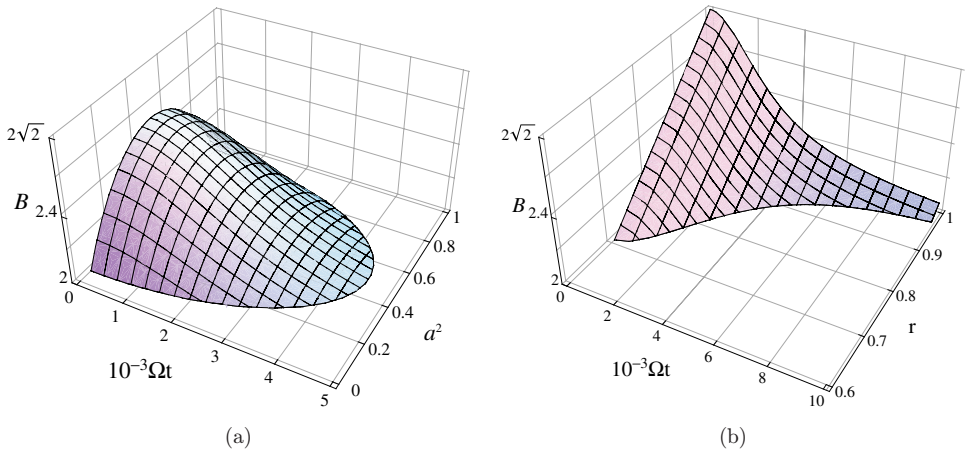


Fig. 1. Maximum of the Bell function,  $B$ , at  $\theta = \pi/2$  and  $\Sigma/\Omega = 0.02$  under adiabatic (low frequency) noise. Panel (a)  $B$  as a function of dimensionless time  $\Omega t$  and  $|a|^2$  ( $r = 0.9$ ); Panel (b)  $B$  as a function of dimensionless time  $\Omega t$  and  $r$  ( $a = 1/\sqrt{2}$ ).

## 5.2. Interplay of adiabatic and quantum noise

We now analyze the interplay of adiabatic and quantum noise simultaneously affecting the two units.

When quantum noise (high-frequency,  $f \sim \Omega$ ) is included, it adds up to the defocusing channel leading to both extra exponential decay of the coherences and evolution of the populations. This is due to the fact that, in practical situations, decay rates are much less sensitive than phases to fluctuations of control parameters. Single-qubit populations are obtained by the Born-Markov master equation. They decay with a relaxation rate  $T_1^{-1} = S_f(\Omega)/2$  to asymptotic values which depend in general on  $\Omega$  and on temperature  $T$ .<sup>25</sup> For typical values of  $\Omega$  ( $\sim 10^{11}$  rad/s) and  $T$  ( $\sim 0.04$  K), asymptotic values of the excited,  $|4\rangle$ , and of the ground state,  $|1\rangle$ , populations are practically zero and one, respectively. On the other hand, the coherences acquire an additional exponential decaying factor.<sup>24,25</sup> Using the reported single-qubit density matrix elements for this case,<sup>24</sup> we construct the new two-qubit density matrix<sup>33,25</sup> from which we determine  $B(t)$ . The maximum of the Bell functions for the two initial EWL states are now formally nonequivalent, this is a qualitative difference with the adiabatic noise case. However, for the typical experimental parameters involved in such nanosystems, quantitatively they do not differ significantly (their difference being always  $\lesssim 10^{-3}$  in the violation region). We are interested to the VSD times  $t_{\text{VSD}}$  when  $B = 2$ . These times are plotted in Fig. 2 as a function of the purity  $r$  for fixed  $a = 1/\sqrt{2}$  (maximally entangled pure part), with noise parameters having values retrieved in experiments.<sup>12,21</sup> In particular, the white noise level is  $S_f = 2 \times 10^6 \text{s}^{-1}$ . We distinguish the cases of only adiabatic noise, only quantum noise and their interplay. For  $r < 1$ , adiabatic noise suppresses nonlocal

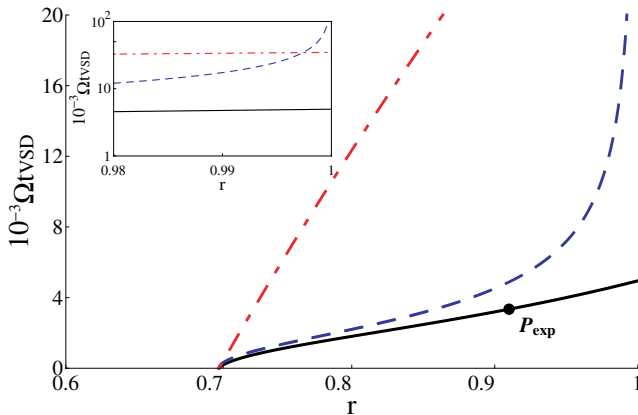


Fig. 2. Dependence of the VSD time on the purity  $r$  ( $a = 1/\sqrt{2}$ ) for initial state  $\hat{\rho}^\Psi$ . The behavior for  $\hat{\rho}^\Psi$  is also quantitatively similar. The blue dashed curve is  $\Omega t_{\text{VSD}}^{\text{ad}}$ , red dot-dashed curve is for quantum noise, black curve is the result of adiabatic and quantum noise altogether. Noise parameters are  $\Sigma = 0.02\Omega$ ,  $S_f(\omega) = 2 \times 10^6 \text{s}^{-1}$ . In addition,  $\Omega = 10^{11}$  rad/s,  $\theta = \pi/2$ ,  $T = 0.04$  K. The inset zooms the region where  $r \approx 1$ . The point  $P_{\text{exp}}$  corresponds to  $r_{\text{exp}} \approx 0.91$  where  $\Omega t_{\text{VSD}} \approx 3350$ .

correlations on a much shorter time scale than quantum noise. For high purity levels, the VSD time due to quantum noise is instead shorter than the adiabatic VSD time (inset of Fig. 2), which goes to infinity for pure states (see Eq. (6)). However, a quantitative estimate of the amount of nonlocal correlations preserved before  $B = 2$  indicates that, for typical amplitudes of  $1/f$  and white noise, adiabatic noise considerably reduces the amount of nonlocal correlations on a short time scale even for  $r \rightarrow 1$ . A finite value of  $t_{\text{VSD}}$  is ensured for *any* initial state only because of quantum noise.

### 5.3. Maximum of the Bell function versus concurrence

Here we compare the dynamics of the maximum of the Bell function  $B$  with the evolution of the concurrence  $C$ , so to establish their connection in such a solid-state system. We consider initial preparation in the two Bell states  $|\Phi\rangle = (|01\rangle + |10\rangle)/\sqrt{2}$  and  $|\Psi\rangle = (|00\rangle + |11\rangle)/\sqrt{2}$ . The behavior for different initial values of  $a$  and  $r$  does not differ qualitatively. Remarkably, for the considered system there is a one-to-one correspondence between  $B$  and  $C$  during the dynamics for both initial states, as shown in Fig. 3. This property has already been observed in other physical contexts<sup>39,41</sup> (atomic qubits in cavities). However, the common behavior for both initial states is not predictable a priori. In general, it may strongly depend on the physical system and on the specific initial state.<sup>39</sup>

The slightly different time dependence for the two Bell states is evidenced by the different distance along the curves of the dots pointing to times  $10^{-3}\Omega t = i$  ( $i = 1, \dots, 5$ ). In addition, the threshold value of  $C$  below which there is no violation anymore is clearly visible. Starting from the initial state  $|\Phi\rangle(|\Psi\rangle)$  we find that for  $C \leq 0.43$  ( $C \leq 0.38$ ) the maximum of the Bell function  $B \leq 2$ , so that we cannot be sure of the presence of nonlocal correlations in this region.

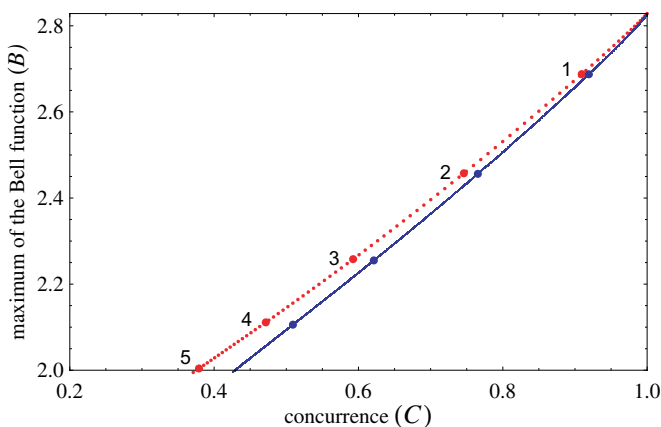


Fig. 3. Maximum of the Bell function  $B$  versus concurrence  $C$  for the two initial Bell states  $|\Phi\rangle$  (blue solid curve) and  $|\Psi\rangle$  (red dotted curve) in the presence of both adiabatic and quantum noise. The points on the curves labeled with  $i = 1, 2, \dots, 5$  indicates the values of  $(C, B)$  at times  $10^{-3}\Omega t = i$ .  $B$  for  $|\Phi\rangle$  decays a little bit faster than that for  $|\Psi\rangle$ . Noise parameters as in Fig. 2.

## 6. Conclusion

In this paper we have investigated the time evolution of nonlocal correlations (nonlocality), identified by the maximum of the Bell function  $B$  when it violates the CHSH-Bell inequality ( $B > 2$ ), between two noninteracting Josephson qubits subject to independent baths with broadband noise typical of solid state nanosystems. In particular, an adiabatic (low-frequency) noise and a quantum (high-frequency) noise can be distinguished. We have shown that, while adiabatic noise has the main effect on nonlocality decay, it is the quantum noise that induces a complete disappearance of quantum nonlocal correlation for any initial state (even for pure maximally entangled states). In particular, we have also reported the times when  $B = 2$  ( $t_{\text{VSD}}$ ), after which there is no more certainty of the presence of quantum nonlocal correlations. We have finally compared, for this system, the dynamics of nonlocal correlations and that of entanglement, quantified by the concurrence  $C$ . We have found that a one-to-one correspondence between  $B$  and  $C$  occurs in time, independently on the form of the initial two-qubit state. Moreover, we obtained thresholds values of  $C$  below which the Bell inequality is not violated ( $B \leq 2$ ).

The results presented in this paper provide new insights towards the possibility to exploit nonlocal quantum correlations for quantum information processing with superconducting nanocircuits.

## References

1. M. Nielsen and I. Chuang, *Quantum Computation and Quantum Information* (Cambridge Univ. Press, 2005).
2. R. Horodecki *et al.*, *Rev. Mod. Phys.* **81** (2009) 865.
3. H. Ollivier and W. H. Zurek, *Phys. Rev. Lett.* **88** (2001) 017901.
4. J. S. Bell, *Physics* **1** (1964) 195.
5. J. F. Clauser *et al.*, *Phys. Rev. Lett.* **80** (1969) 23.
6. Y. Yu *et al.*, *Science* **296** (2002) 889.
7. J. M. Martinis *et al.*, *Phys. Rev. Lett.* **89** (2002) 117901.
8. F. Deppe *et al.*, *Nature Phys.* **4** (2008) 686.
9. E. Lucero *et al.*, *Phys. Rev. Lett.* **100** (2008) 247001.
10. J. M. Chow *et al.*, *Phys. Rev. Lett.* **102** (2009) 090502.
11. J. A. Schreier *et al.*, *Phys. Rev. B* **77** (2008) 180502(R).
12. D. Vion *et al.*, *Science* **296** (2002) 886.
13. T. Hime *et al.*, *Science* **314** (2006) 1427.
14. J. Majer *et al.*, *Nature* **449** (2007) 443.
15. A. Fay *et al.*, *Phys. Rev. Lett.* **100** (2008) 187003.
16. M. Steffen *et al.*, *Science* **313** (2006) 1423.
17. J. H. Plantenberg *et al.*, *Nature* **447** (2007) 836.
18. S. Filipp *et al.*, *Phys. Rev. Lett.* **102** (2009) 200402.
19. P. J. Leek *et al.*, *Phys. Rev. B* **79** (2009) 180511(R).
20. L. DiCarlo *et al.*, *Nature* **460** (2009) 240.
21. G. Ithier *et al.*, *Phys. Rev. B* **72** (2005) 134519.
22. O. Astafiev *et al.*, *Phys. Rev. Lett.* **93** (2004) 267007.
23. A. Shnirman *et al.*, *Phys. Rev. Lett.* **94** (2005) 127002.



24. G. Falci *et al.*, *Phys. Rev. Lett.* **94** (2005) 167002.
25. B. Bellomo *et al.*, *Phys. Rev. A* **81** (2010) 062309.
26. A. Acin, N. Gisin and L. Masanes, *Phys. Rev. Lett.* **97** (2006) 120405.
27. M. Horodecki, P. Horodecki and R. Horodecki, *Phys. Lett. A* **200** (1995) 340.
28. M. B. Weissman, *Rev. Mod. Phys.* **60** (1988) 537.
29. E. Paladino *et al.*, *Phys. Rev. Lett.* **88** (2002) 228304.
30. E. Paladino *et al.*, *Adv. Solid State Phys.* **43** (2003) 747.
31. Y. M. Galperin *et al.*, *Phys. Rev. Lett.* **96** (2006) 097009.
32. E. Paladino *et al.*, *Phys. Scr.* **T137** (2009) 014017.
33. B. Bellomo, R. Lo Franco and G. Compagno, *Phys. Rev. Lett.* **99** (2007) 160502.
34. B. Bellomo, R. Lo Franco and G. Compagno, *Phys. Rev. A* **77** (2008) 032342.
35. E. Hagley *et al.*, *Phys. Rev. Lett.* **79** (1997) 1.
36. P. G. Kwiat *et al.*, *Nature* **409** (2001) 1014.
37. J. S. Pratt, *Phys. Rev. Lett.* **93** (2004) 237205.
38. B. Bellomo, R. Lo Franco and G. Compagno, *Phys. Lett. A*, in press (2010). Also quant-ph/0910.3861.
39. L. Mazzola *et al.*, *Phys. Rev. A* **81** (2010) 052116.
40. A. Miranowicz, *Phys. Lett. A* **327** (2004) 272.
41. B. Bellomo, R. Lo Franco and G. Compagno, *Phys. Rev. A* **78** (2008) 062309.
42. W. K. Wootters, *Phys. Rev. Lett.* **80** (1998) 2245.